Femtosecond Optical Pump–Probe Characterization of High-Pressure–Grown $Al_{0.86}Ga_{0.14}N$ Single Crystals

The group-three–nitride (III-N) semiconducting system, in general, and (Al,Ga)N compounds, in particular, have attracted a very strong interest in recent years for the development of optoelectronic devices from the green to deep-ultraviolet wavelength range.[1] Moreover, III-N materials have also well-documented advantages in high-temperature and high-power electronics, as well as in acoustic-wave applications.[2–4] A considerable amount of research has been devoted to the epitaxial growth of (Al,Ga)N films, using MOCVD and/or MBE methods.[5,6] The growth of bulk, dislocation-free (Al,Ga)N crystals is also critical not only for getting much-needed single-crystal substrates for homoepitaxy, but also for applications where the devices operate based on the volume-absorption principle, e.g., x-ray and other radiation detectors. Unfortunately, the growth of even small, high-quality (Al,Ga)N single crystals, especially those with the high Al content, is very challenging, and only very recently, the synthesis of $Al_xGa_{1-x}N$ crystals with the Al content x between 0.5 and 1 has been reported by Belousov *et al.*[7]

In this article, we report our femtosecond, time-resolved pump–probe spectroscopy studies in $Al_{0.86}Ga_{0.14}N$ (AlGaN) single crystals and demonstrate that the observed transient transmissivity signal is a superposition of the femtosecond correlation signal caused by a coherent process of simultaneous absorption of both the pump and probe photons and a conventional, picosecond-in-duration hot-electron cooling. The pump–probe correlation studies, typically called a two-photon absorption (TPA) process, are important in nonlinear optics and have been investigated in many semiconducting materials, such as GaAs, GaN, and (In,Ga)N;[8] the large magnitude of the TPA coefficients β are reported in Ref. 9. Moreover, the TPA measurement is a useful tool for characterizing optical pulse widths and determining the optical energy gap in wide-bandgap semiconductor materials. At the same time, the photoresponse relaxation transient, which in our case follows the initial correlation spike, provides information about the electron–phonon decay time and the across-bandgap carrier recombination.

Our single AlGaN crystals used in this study were synthesized from solution at high temperatures using a high-pressure gas system, which consists of a compressor, pressure intensifier, and a high-pressure chamber of 40-mm internal diameter with an internal, three-zone furnace. First, a polycrystalline (Al,Ga)N precursor pellet was synthesized by a solid-phase reaction in a cubic anvil at 30 kbar and 1800°C from a mixture of high-purity GaN and AlN powders (Alfa Ceasar). The prereacted pellet acted as an Al source and was placed in the Ga melt in the upper part of a graphite crucible. The graphite crucible had an internal diameter of 14 mm and a length of 70 mm. For the AlGaN crystal growth, we applied a nitrogen pressure of up to 7.5 kbar and a temperature of up to 1760°C, following our earlier, experimentally derived pressure-versus-temperature diagram.[7] The synthesis process was conducted under the constant thermal gradient of about 20 K/cm for 6 to 7 days. The crystals grown in the colder part of the graphite crucible were colorless, up to $0.8 \times 0.8 \times 0.8$ mm^3 in size, and exhibited the hexagonal form and wurtzite structure. After processing, the samples were etched from the remaining unreacted Ga/Al melt using hydrochloric acid and *aqua regia*. The structural composition was determined by a laser-ablation, inductively coupled plasma mass spectrometry technique.

Our time-resolved photoresponse studies were performed in a transmission configuration, using a two-color, femtosecond pump–probe technique. We used a passively mode-locked Ti:sapphire laser as a source of 100-fs-wide, 76-MHz-repetition-rate optical pulses, tunable in the 720- to 860-nm range. The Ti:sapphire output was split into two beams by a 60/40 beam splitter. The pump beam, frequency doubled by using a BaB_2O_4 crystal, was focused onto the surface of the AlGaN crystal with a spot diameter of ~100 μm at an incident angle of ~20°. The probe pulses, directly generated by the Ti:sapphire laser, were delayed with respect to the pump by passing through a computer-controlled delay stage and were near normally aimed at the sample on the same area as the pump beam with a spot diameter of ~10 μm. The small spot size of the probe

beam ensured that it probed a region with uniform pump photoexcitation and somewhat relaxed the stringent requirement for the delay-stage alignment. The probe light transmitted through the sample was filtered from any scattered pump photons by a near-infrared filter and collected by a photodetector. The photodetector signal was measured by a lock-in amplifier, synchronized with an acousto-optical modulator operating at frequency of 99.8 KHz. We stress that in our experiments both the pump and probe beams had an average power incident on a sample of a same order (with a typically used ratio $P_{\text{pump}}/P_{\text{probe}}$ of 1:2) and their photon energies were much smaller than the expected ~6-eV bandgap of our AlGaN sample. All experiments were performed at room temperature.

Figure 120.48 presents a typical time-resolved normalized differential transmissivity ($\Delta T/T$) transient, obtained by exciting our AlGaN crystal with a 380-nm pump and probed with a 760-nm probe. Figure 120.48(a) depicts the full transient in a long-time window, and the dashed line is a numerical fit, which will be described later. We observe an initial (near-zero delay), subpicosecond-in-duration negative spike, followed by a much-slower exponential decay. In Fig. 120.48(b), we show the same waveform (solid squares), but on a much-shorter (<3 ps) time scale, and note that the experimental $\Delta T/T$ transient can be very accurately decomposed into a Gaussian-shaped pulse (open triangles) of a full width at half maximum (FWHM) of 310 fs and a second transient (open circles) with an approximately 1-ps-wide rise time, modeled as the error function, and a slow [on the scale of Fig. 120.48(b)] exponential decay. The superposition of the above two transients (open squares) fits our experimental data extremely well [see also dashed line in Fig. 120.48(a)].

Based on our decomposition procedure, we can interpret the ultrafast Gaussian pulse as a TPA-type correlation signal since the 310-fs FWHM coincides well with the overlap of our ~150-fs-wide pump and probe pulses. The TPA signal can be observed only when both the pump and probe photons are simultaneously incident on the sample and their total energy is greater than the material's bandgap E_g. Therefore, we must conclude that in our case, the correlation effect actually involves three photons (one pump photon and two probe photons) since any other combination would give a total photon energy that would be either much too large or too low. The second, slow component of the experimental transient is a typical $\Delta T/T$ pump–probe photoresponse signal, associated in direct-bandgap semiconductors (i.e., in III-N materials) with across-the-bandgap electron-hole excitation, followed by a subsequent cooling of photo-induced electrons. On a long time scale, the relaxation component of the $\Delta T/T$ transient can be fitted [Fig. 120.48(a) (dashed line)] as a bi-exponential decay with an initial 12-ps time constant, followed by a slow, ~130-ps-

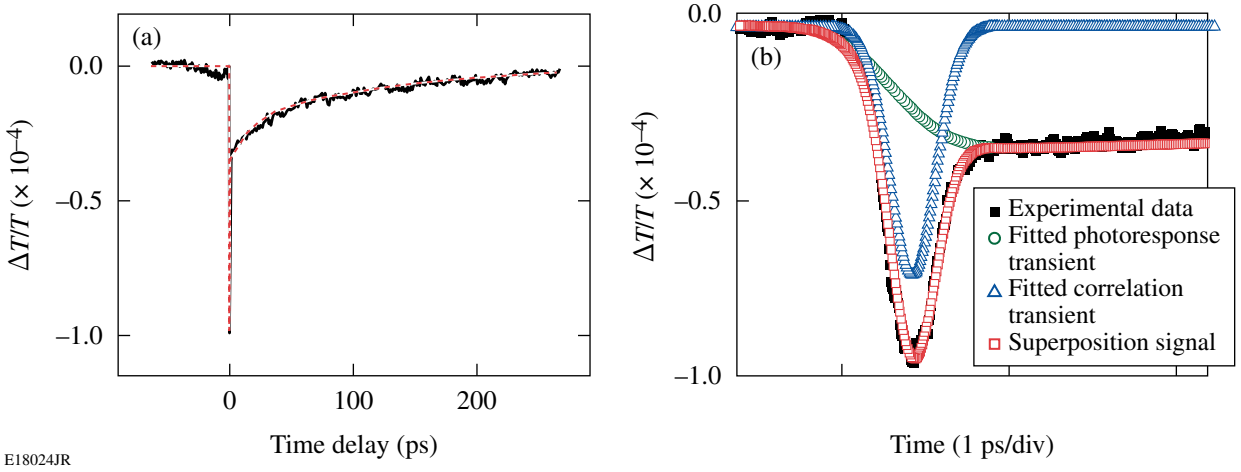

Figure 120.48
(a) Time-resolved $\Delta T/T$ transient measured for the pump λ = 380 nm and the probe λ = 760 nm. The red dashed line represents a theoretical fit. (b) The same $\Delta T/T$ transient (black squares), but on a much-shorter time scale. The blue triangles are the best fit corresponding to a Gaussian-shaped correlation signal of the pump and probe photons. The green circles fit the photoresponse component of the transient, with the rising part represented by the error function and the decay modeled as a double-exponent relaxation. The red squares correspond to the superposition of the correlation and photoresponse components and overlay the experimental data. The fit of the red squares in (b) is identical to the red dashed line in (a).

long relaxation. The fast decay time constant represents the electron–phonon relaxation process toward a quasi-equilibrium condition at the bottom of the conduction band, while the slow time constant is the carrier lifetime, which includes both the radiative (across the bandgap) and nonradiative (trapping) recombination.

We have also studied the amplitude dependence of the photon-correlation signal deconvoluted from the experimental $\Delta T/T$ transient on the pump power's density (see Fig. 120.49) and have found that, in the regime of low attenuation of the incident pump and probe beams, it followed a linear behavior, well-established for the TPA process:[10]

$$\Delta T/T = -\beta d P_{\text{eff}}, \tag{1}$$

where d is the sample thickness and P_{eff} is the effective, absorbed pump-beam power per pulse. The data presented in Fig. 120.49 were collected for the pump-beam wavelength λ = 380 nm and d = 1 mm. Using Eq. (2) and taking into account that in our experiment the pump spot diameter is 100 μm and its absorption coefficient is ~80%, the linear fit (solid line) in Fig. 120.49 allowed us to calculate β = 0.42±0.02 cm/GW. We note that our β value is significantly smaller than the ones observed in other III-N materials [e.g., for GaN, β = 12 cm/GW at 377 nm (Ref. 8)], apparently due to a much larger E_g value for (Al,Ga)N.

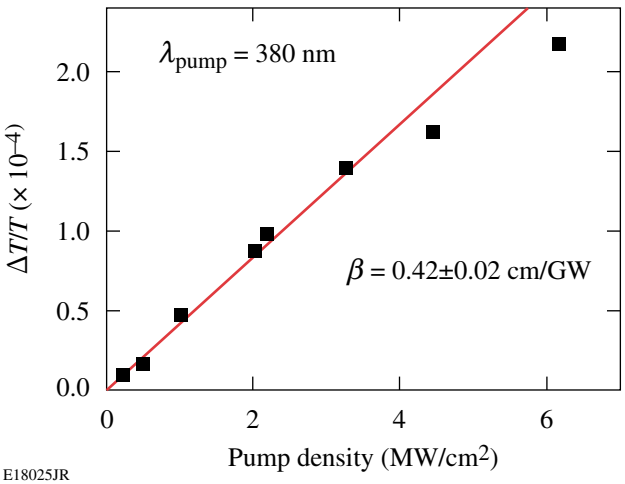

Figure 120.49
Dependence of the correlation signal amplitude (squares) on the pump power's intensity, measured for a 380-nm pump wavelength. The solid red line is the linear best fit and its slope corresponds to the β coefficient.

Following the procedure discussed in connection with Fig. 120.49, we obtained β coefficients for the pump λ's ranging from 360 nm to 430 nm. The results (solid circles) are summarized in Fig. 120.50 and compared directly with the theoretical model of Sheik–Bahae *et al.*,[11] derived for wide, direct-bandgap semiconductors:

$$\beta(\omega) = K\frac{\sqrt{E_p}}{n_0^2 E_g^3} F_2\left(\frac{\hbar\omega}{E_g}\right), \tag{2}$$

where K is a material-independent constant, E_p is the matrix element related to the interband momentum and is ~21 eV for most semiconductors, n_0 is the refractive index, and the $F_2\left(\hbar\omega/E_g\right)$ function is given as $F_2 = (2x-1)^{3/2}/(2x)^5$.

In our case, K = 3100, E_g = 5.81 eV (from our bandgap measurement presented below), and n_0 is a function of λ and for our AlGaN sample is given by $n_0(\lambda) = 2.02 + 4.7e^{-\lambda/93.86}$ (Ref. 5). We observe a very good agreement of our experimental β values with the Sheik–Bahae model, within the pump light λ's achievable by our experimental setup. The inset in Fig. 120.50 presents a subset of the same data (β values very close to zero) as the main panel, but plotted as a function of total energy of photons incident on our sample and participating in the pump–probe correlation process (one pump photon and two probe photons). In this way, we can observe the optical

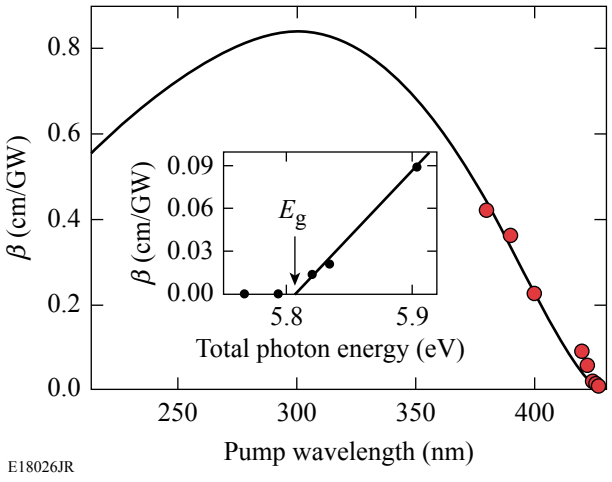

Figure 120.50
The correlation coefficient β as a function of the pump beam's wavelength. The red circles are our experimental data points, while the solid line corresponds to the Sheik–Bahae theory [Eq. (3)]. The inset shows β dependence on the total energy of absorbed photons with the optical bandgap absorption edge indicated.

transition edge in detail, and a simple linear fit allows us to very accurately determine the optical E_g of our AlGaN crystal to be equal to 5.81±0.01 eV.

We have performed time-resolved characterization of AlGaN single crystals using femtosecond pump–probe spectroscopy with both the pump and probe beams having wavelengths much longer than the wavelength corresponding to the AlGaN bandgap. Examination of our experimental data showed that two different processes contributed simultaneously to the $\Delta T/T$ transients observed on our experiments. The first was the ~300-fs-wide correlation signal, observed near the zero-delay point and corresponding to the photon correlation process involving a coherent (simultaneous) absorption of one pump and two probe photons. It was followed by a second, much slower (tens of picosecond in duration) relaxation transient representing photoresponse and cooling of photo-excited carriers. Analysis of the correlation signal amplitude on both the pump photon power and wavelength allowed us to obtain the correlation β coefficient for our AlGaN crystal and its spectral dependence. We demonstrated that, within our laser-tuning range, $\beta(\lambda)$ agreed very well with the Sheik–Bahae theory. We also determined that the optical E_g of AlGaN was 5.81±0.01 eV. The dynamics of the photoresponse decay component demonstrated that the carrier relaxation in AlGaN was dominated by trapping since the measured 130-ps time constant was relatively short.

ACKNOWLEDGMENT

The authors would like to thank Prof. D. Günther from the Laboratory for Inorganic Chemistry, ETH Zurich, for his assistance in (Al,Ga)N mass spectrometry characterization. J. Z. acknowledges support from the Frank Horton Graduate Fellowship Program at the University of Rochester Laboratory for Laser Energetics, funded by the U.S. Department of Energy Office of Inertial Confinement Fusion under Cooperative Agreement No. DE-FC52-08NA28302 and the New York State Energy Research and Development Authority. The support of DOE does not constitute an endorsement by DOE of the views expressed in this article.

REFERENCES

1. S. N. Mohammad, A. A. Salvador, and H. Morkoc, Proc. IEEE **83**, 1306 (1995).
2. Q. Chen *et al.*, Appl. Phys. Lett. **70**, 2277 (1997).
3. U. K. Mishra *et al.*, Proc. IEEE **96**, 287 (2008).
4. S. Wu, P. Geiser, J. Jun, J. Karpinski, J.-R. Park, and R. Sobolewski, Appl. Phys. Lett. **88**, 041917 (2006).
5. M. Stutzmann *et al.*, Mater. Sci. Eng. B **B50**, 212 (1997).
6. Y. Koide *et al.*, J. Appl. Phys. **61**, 4540 (1987).
7. A. Belousov, S. Katrych, J. Jun, J. Zhang, D. Günther, R. Sobolewski, and J. Karpinski, J. Cryst. Growth **311**, 3971 (2009).
8. C.-K. Sun *et al.*, Appl. Phys. Lett. **76**, 439 (2000).
9. S. Krishnamurthy, K. Nashold, and A. Sher, Appl. Phys. Lett. **77**, 355 (2000).
10. C. Rauscher and R. Laenen, J. Appl. Phys. **81**, 2818 (1997).
11. M. Sheik-Bahae *et al.*, IEEE J. Quantum Electron. **27**, 1296 (1991).